An investigation of planar array system artefacts generated within an electrical impedance mammography system developed for breast cancer detection

Article (Published Version)

An Investigation of Planar Array System Artefacts Generated within an Electrical Impedance Mammography System Developed for Breast Cancer Detection

Rabia Bilal[1] , Rupert Young[2] , Chris Chatwin[3], Bilal Muhammad Khan[4]

[1,2,3]Department of Engineering and Design, University of Sussex UK.

[4]Department of Electronic and Power Engineering, PNEC, National University of Sciences and Technology (NUST), Karachi, Pakistan

rabiabilal05@gmail.com[1],r.c.d.young@sussex.ac.uk[2],C.R.Chatwin@sussex.ac.uk[3], bmkhan@pnec.nust.edu.pk[4]

Abstract

An Electrical Impedance Mammography (EIM) planar array imaging system is being developed at the University of Sussex for the detection of breast cancers. Investigations have shown that during data collection, systematic errors and patient artefacts are frequently introduced during signal acquisition from different electrodes pairs. This is caused, in particular, by the large variations in the electrode-skin contact interface conditions occurring between separate electrode positions both with the same and different patients. As a result, the EIM image quality is seriously affected by these errors. Hence, this research aims to experimentally identify, analyse and propose effective methods to reduce the systematic errors at the electrode-skin interface. Experimental studies and subsequent analysis is presented to determine what ratio of electrode blockage seriously affects the acquired raw data which may in turn compromise the reconstruction. This leads to techniques for the fast and accurate detection of any such occurrences. These methodologies can be applied to any planar array based EIM system.

Keywords

Breast Cancer Detection; Electrical Impedance Tomography; Contactless Electrode Artefacts; Infinite Impedance, Planar Eim System.

Introduction

Breast cancer is a significant healthcare problem and a leading cause of death in women in the World (American Cancer Society 2009). Electrical Impedance Tomography (EIT) is a non-invasive imaging technique researched for clinical use (Barber and Brown 1984) by which images of the internal impedance distribution of the human body can be reconstructed mathematically from voltage measurements made by electrodes placed on the skin (Holder D S 2005). It has advantages of low cost, a non-invasive nature and the ability to characterise human tissue types through their measured electrical properties. These characterising abilities are an exclusive feature among all other screening technologies such as ultrasound, Magnetic Resonance Imaging and Computed Tomography. However, impedance-based tomography techniques have suffered from relative inaccuracy due to practical problems with electrode-skin contact (Boone 1996, Kolehmainen *et al* 1997, Nissinen *et al* 2009).

The Sussex Electrical Impedance Mammography (EIM) Mark 4 System uses a 'wet' electrode structure (Huber N *et al* 2010), as shown in figure 1, which allows indirect contact between the skin and electrodes through a dielectric medium, helping in the reduction of contact impedance.

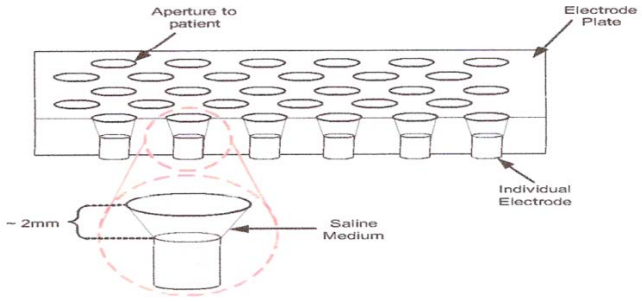

FIGURE 1. THE SUSSEX MK 4 EIM SYSTEM WET PATIENT-ELECTRODE INTERFACE WITH "NO-CONTACT" DESIGN (HUBER N *ET AL* 2010)

The breast to be imaged extends through an opening into a plastic, cylinder-shaped scanner head filled with a body-temperature saline liquid, the patient lying comfortably face down on an examination table.

Fixed at the bottom of the saline filled cylinder is an 84 electrode planar array plate which is adjusted according to different breast sizes so that the breast comes into contact with it partially compressed. The plate is embedded in a sealed plastic housing that contains the driving circuitry and the digitally controlled switching circuitry. To satisfy our clinical requirement, a safe AC current not exceeding 1mA is employed with a signal frequency ranging from 10 kHz to 10 MHz.85 electrodes are arranged in an hexagonal pattern and are positioned equal distances of 17mm from each other. 122 different injection drive patterns are used giving a total of 1416 measurements. Each drive requires 10 to 12 voltage measurements per frame. The switching of the electrodes for each frame is driven by a multiplexing arrangement (Sze G *et al* 2011).

Measurement frames of the Sussex hexagon planar array have 10 or 12 numbers of points. 10 point measurement frames are known as non-symmetrical, whereas the 12 point measurement frames are defined as symmetrical. Non-symmetrical frames tend to be on the corners. Symmetrical frames have 12 measurement points and are considered to be in the central area shown in figure 2. Due to the non-symmetrical nature of the frames on the corners, breast localisation somewhere in the middle of the planar array electrode is important.

As electrode-skin contact artefacts are amplified by the use of inverse problem solutions for imaging, electrode blocking introduces artefacts in the reconstructed conductivity images with a greater effect in absolute imaging, as the forward solution depends on the electrode skin contact impedance (Mc Ewan *et al* 2007, Boone *et al* 1996,Cheng *et al* 1989, Paulson *et al* 1992, McAdams *et al* 1996, Wang *et al* 2007, Rahal *et al* 2009)

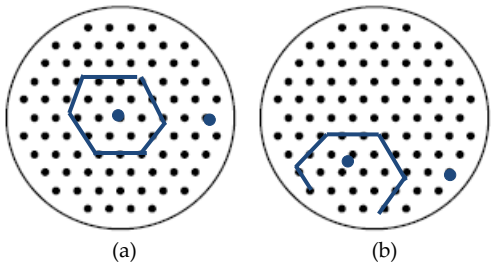

FIGURE 2:(A) SYMMETRICAL FRAME DRIVE-ELECTRODES FOR A MAXIMUM 12 MEASUREMENTS (BLUE HEXAGON) (B) NON-SYMMETRICAL FRAME WITH 10 MEASUREMENTS.

While analysing the clinical data(Huber N *et al* 2010) it has been noticed that at certain electrode combinations the acquired signal response is either saturated or zero. Complete electrode blockage results in dead or saturated signals on the particular electrode combination. EIM will thus become challenging for clinical use since the image reconstruction is susceptible to these errors introduced from data collection. This paper considers a number of possible factors responsible for these unwanted effects. A comprehensive study and analysis is made of what ratio of electrode blockage can affect the acquired raw data and thus compromise the reconstruction that follows. Techniques are proposed for the fast detection of any such occurrences.

Planar Electrode Array Artefacts

Artefacts introduced by the patients and the patient-electrode interfaces are the main challenges faced by the EIM technology. These artefacts not only affect the repeatability and accuracy of the system performance but also the reconstructed image quality. The patient electrode interface (Huber N *et al* 2010, Beqo N *et al* 2011) is the most important and challenging aspect to be investigated in detail. Undesired threshold voltage levels between the acquired measurement frames will be the cause of artefacts in the reconstructed conductivity images (Hua P *et al* 1993). Infinite impedance due to electrode blockage is a factor in the occurrence of these abnormal measurements. The infinite impedance effect is more marked in absolute imaging, as the forward reconstruction solution is strongly reliant on the electrode-skin contact impedances (Kolehmainen *et al* 1997, Nissinen *et al* 2009).

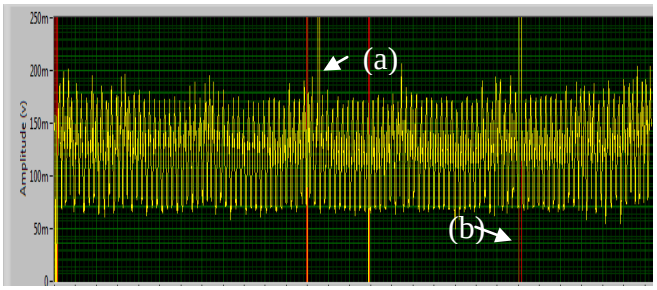

FIGURE 3. DEAD AND SATURATED ELECTRODE COMBINATIONS : (A) SATURATED (B) DEAD

The acquired signal when measured showed saturated or dead channels in the presence of bubbles or other electrode blockages as indicated in figure 3.Impedance representations of saturated and dead channels are shown in figure 4 (a) and (b) which indicate the disrupted channels in red.

Possible factors inducing the occurrence of infinite impedance such as patient introduced errors,

electrolysis and sensor configuration are discussed below. This discussion is supported by generating the same the sensor responses with a phantom and syringe to locally inject air bubbles as well as determining what percentage of the 2mm of electrode size needs to be contacted to generate a usable signal.

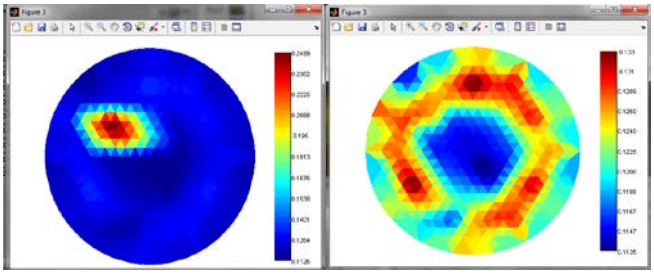

(a) (b)

FIGURE 4. 2D IMPEDANCE IMAGE INDICATING: (A) SATURATION AT THE 10 O'CLOCK POSITION AND (B) DEAD CHANNELS (THE RING IN RED).

Patient Introduced Errors

Air remains trapped as small bubbles in the fine hair of dry skin when immersed in the saline solution with which the receiving chamber of the EIM system is filled. This generates an insulating layer and so disrupts the signals from electrodes located under these regions.

Also, direct skin-electrode contact is a further problem that will cause errors. Thus the partial compression of the breast onto the sensor plate during the scanning process causes saline to displace from the 2mm electrode cavities (Huber N *et al* 2010). Experiments carried out on volunteers for the Sussex Mk_4 System showed saturated measurements together with very low or zero signal levels in some regions of the acquired data. This condition varied with the subject under examination making it obvious that the problem is not something that is associated with systematic errors. A possible reason for these unwanted acquired voltage levels is the weight of the subject's breast removing the interfacing saline medium and so producing a direct contact between the skin and the electrode.

Electrolysis

Electronic circuits connected to the electrodes can possibly cause frequency dependent DC offset resulting in bubble generation on the immersed electrodes. This DC offset can be generated during switching of the electrodes, or by electrodes not used for injection but for acquiring a signal at that point. As the DC signal passes through and between the electrodes, the saline solution splits into hydrogen and chlorine gas, which collects as very tiny bubbles around, and on, the electrode. There are a number of ways to reduce any DC offset by careful design of the front-end electronics link to the electrodes. However, the DC offset will remain, at some level, between the electrodes.

The generated bubbles cover some ratio of the electrode area; the extent of this that affects the acquired voltages has been determined and is discussed in this paper.

Sensor Error

While investigating the mechanisms of bubble generation, it was observed that the bubbles are generated if the `dry` scanner head is filled with a dielectric medium before scanning. These bubbles keep on growing because of the micro gaps between the sensors and the acrylic plate. Different sizes of the bubbles generated on the electrodes will at some ratio block the electrode, so affecting the acquired voltages.

Problem Analysis and Discussion

This section investigates at what ratio of blockage of the 2mm electrode it is that the unwanted threshold voltage levels occur that are responsible for artefacts appearing in the reconstructed conductivity images (Sze G *et al* 2011). To accomplish this, different sizes of bubbles were artificially introduced on to the driving and receiving electrodes to provide a forced blocking, as shown in figure 5. Bubbles covering 1/8, 1/4, 1/2 and the full electrode diameter were artificially introduced using a syringe. This experiment was carried out by filling the scanner head with room temperature saline of 0.5mS/cm conductivity.

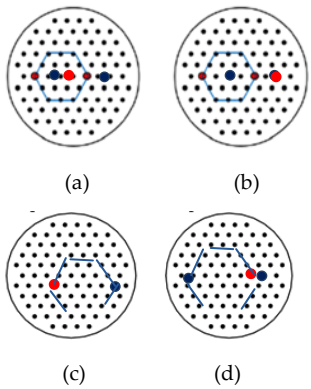

(a) (b)

(c) (d)

FIGURE 5. (A) SYMMETRICAL FRAME DRIVE - FULLY BLOCKED RECEIVING ELECTRODE (IN RED) (B) SYMMETRICAL FRAME DRIVE - FULLY BLOCKED DRIVING ELECTRODE (IN RED) (C) NON-SYMMETRICAL FRAME DRIVE - FULLY BLOCKED RECEIVING ELECTRODE (IN RED) (D) SYMMETRICAL FRAME DRIVE - FULLY BLOCKED DRIVING ELECTRODE (IN RED).

Analysis of the results are carried out in two stages. Firstly, comparison is done with the symmetrical frame threshold levels at different acquisition frequencies (50 kHz and 500 kHz) with the electrodes blocked to certain defined ratios.

Secondly, a set of comparisons is carried out on the receiving and driving electrodes with symmetrical and non-symmetrical frames by comparing different threshold levels caused by the different ratios of electrode blockage, again at both 50 kHz and 500 kHz acquisition frequencies.

Undesired threshold voltage levels between the acquired symmetrical and non-symmetrical measurement frames introduce artefacts in the reconstructed conductivity images.

Summarised results of the driving and receiving electrode symmetrical frames are shown in table 1 and table 2, respectively, to indicate the undesired threshold levels.

TABLE 1. COMPARATIVE ANALYSIS OF DIFFERENT BUBBLE SIZES ON THE DRIVING ELECTRODE.

Frequency	Bubble Size	SNR_{max} (dB)	SNR_{min} (dB)	V_{max} (mV)	V_{min} (mV)
50KHz	1/8	39.49	32.98	368	174
	1/4	40.47	35.33	345	203
	1/2	40.89	31.29	387	180
	Full	11.00	06.00	012	004
	No bubble	40.34	33.71	383	183
500KHz	1/8	27.84	19.39	098	042
	1/4	27.84	19.38	099	042
	1/2	30.12	22.74	112	051
	Full	10.42	04.67	010	004
	No bubble	29.27	21.82	115	053

TABLE 2. COMPARATIVE ANALYSIS OF DIFFERENT BUBBLE SIZES ON THE RECEIVING ELECTRODE.

Frequency	Bubble Size	SNR_{max} (dB)	SNR_{min} (dB)	V_{max} (mV)	V_{min} (mV)
50KHz	1/8	39.49	32.98	368	174
	1/4	40.47	35.33	345	203
	1/2	40.89	31.29	387	180
	Full	40.56	35.67	0.0022	179
	No bubble	40.34	33.71	383	183
500KHz	1/8	27.84	19.39	098	042
	1/4	27.84	19.38	099	042
	1/2	30.12	22.74	112	051
	Full	30.23	04.67	0.0022	004
	No bubble	29.27	21.82	115	053

From the results shown in figures 6(a) and (b), 7(a) and (b) and 8 (a) and (b), it is clear that the maximum impedances, causing the voltage threshold levels to drift to abnormality, are generated by the fully and half blocked electrodes.

Results shown in figure 6 (a) and (b) indicate that the infinite impedance has been introduced due to the fully blocked driving electrode. A bubble completely blocking a drive electrode will affect current production (since air is an insulator) and thus result in negligible or zero signal being applied. This is then responsible for the receiving frame only recording noise or a minimum signal of approximately 0V.

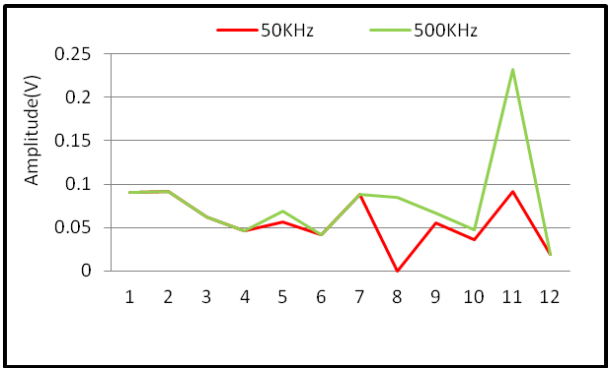

(a)

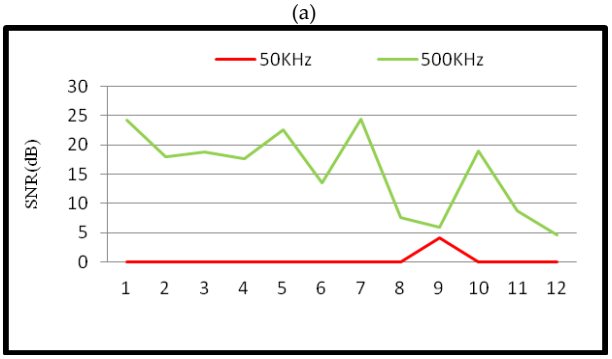

(b)

FIGURE 6. DRIVING ELECTRODE: FULLY BLOCKED. (A)VOLTAGE AMPLITUDE AND (B) SNR

Results shown in figures 7 (a) and (b) and 8(a) and (b) show the acquired threshold levels with the half and fully blocked receiving electrodes, respectively. A saturated response can be observed on position 6 in the measurement frame shown in figure 8(a) and (b). This saturated response is due to the high impedance introduced in the form of a bubble blocking completely the 2 mm acquiring surface. The high impedance point will take an abnormally high voltage drop, referred to as a saturated response in our system. The same position 6 in figure 7 (a) and (b) also indicates the saturated response but with the threshold level half of that at position 6 in figure 8 (a) and (b).

Fully covered driving electrode will disrupt the whole frame of 10 or 12 acquired voltages should be avoided.

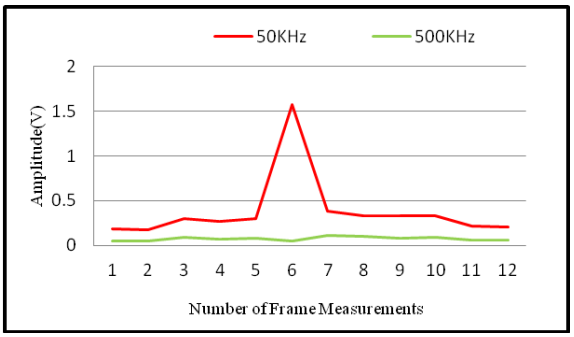

(a)

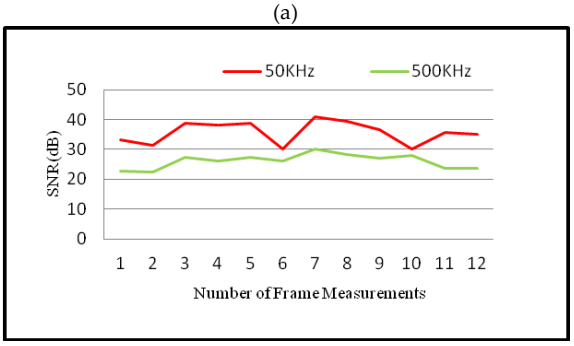

(b)

FIGURE 7.RECEIVING ELECTRODE 1/2 BLOCKED (A) VOLTAGE AMPLITUDE AND (B) SNR

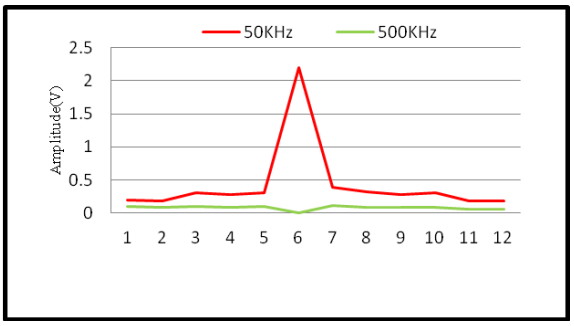

(a)

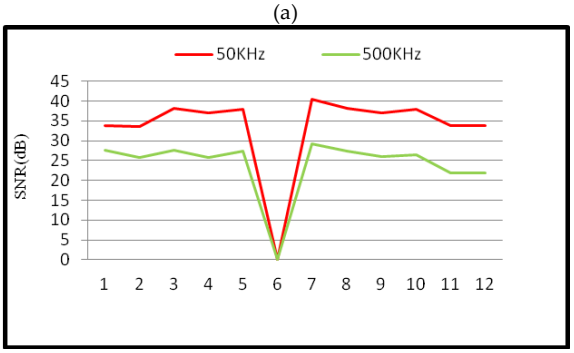

(b)

FIGURE 8. RECEIVING ELECTRODE FULLY BLOCKED (A) VOLTAGE AMPLITUDE AND (B) SNR

Artificially introduced driving and receiving electrode blocking does seem responsible for the abnormal measurements when the electrode is fully covered but does not indicate any undesired threshold levels effects when 1/8, 1/4 and 1/2 of the electrode diameter is covered as indicated in table 1 and table 2.The acquired voltage levels with these ratios of electrode covering are more or less similar to those with no bubble. This indicates that infinite impedance or zero potential is only introduced when the driving electrode or receiving sensor is fully or half blocked.

A second set of comparisons is carried out on the receiving and driving electrodes with the symmetrical and non-symmetrical frames and the results of this comparative study are presented in table 3.

Non symmetrical frames tend to be on the corners and any abnormal response does not appear to affect the whole measurement frame. Due to the non-symmetrical nature of the frames on the corners, breast localisation somewhere in the middle of the planar array electrode is important.

TABLE 3: COMPARATIVE ANALYSIS OF SYMMETRICAL AND NON-SYMMETRICAL DRIVING AND RECEIVING ELECTRODES.

Frequency	Bubble Size	Symmetrical Frame		Non-Symmetrical Frame	
		V_{max}	V_{min}	V_{max}	V_{min}
50KHz	1/8	0.53	0.22	0.64	0.23
	1/4	0.50	0.22	0.64	0.24
	1/2	0.53	0.22	0.63	0.23
	Full	0.10	0.04	0.12	0.02
	No bubble	0.55	0.22	0.65	0.23
500KHz	1/8	0.53	0.22	0.64	0.23
	1/4	0.50	0.22	0.64	0.24
	1/2	1.52	0.22	0.64	0.23
	Full	2.20	0.22	2.20	0.22
	No bubble	0.55	0.22	0.66	0.23

For both symmetrical and non-symmetrical sets of frames, the analysis of the bubbles on the receiving electrode thus shows that the bubbles covering 1/8 and 1/4 of the electrode diameter do not introduce notable impedance, in contrast to the electrodes that are half and fully blocked. A bubble covering a full receiving electrode will introduce very high impedance, resulting in a very large voltage drop (to saturation) as indicated in figure 9 (a) and (b). The voltage measured by the receiving frame will be very small, or almost zero, for the fully blocked driving electrode as shown in figure 10(a) and (b).

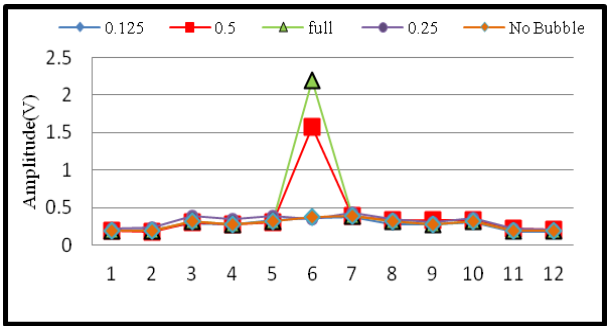

(a)

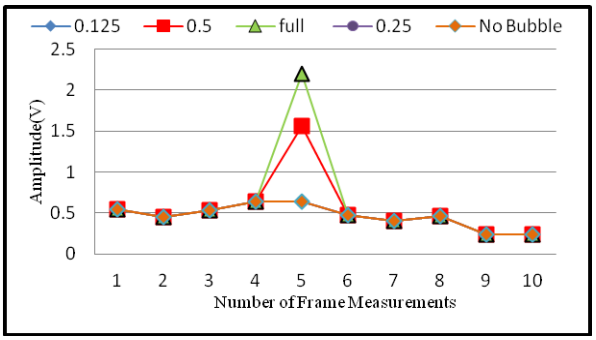

(b)

FIGURE 9. RECEIVING ELECTRODE COMPARATIVE ANALYSIS: (A) SYMMETRICAL FRAME (B) NON-SYMMETRICAL FRAME.

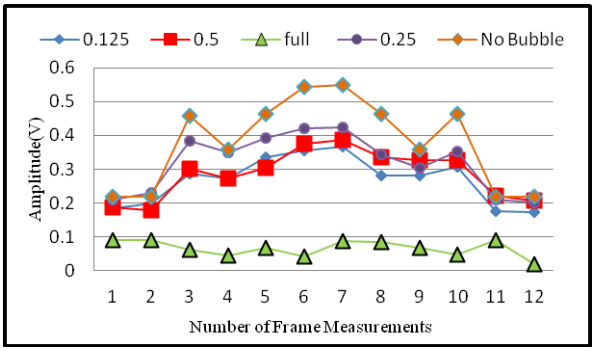

(a)

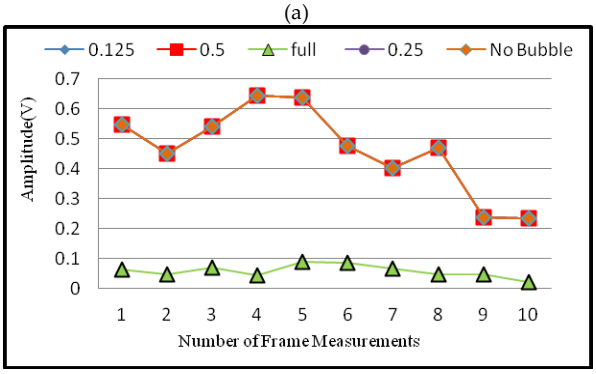

(b)

FIGURE 10. DRIVING ELECTRODE COMPARATIVE ANALYSIS: (A) SYMMETRICAL FRAME (B) NON-SYMMETRICAL FRAME

Artefact Mitigation Methodologies

The artefacts discussed above, and their effect on the acquired signal, need to be addressed in order to obtain better signal quality and subsequent image reconstruction . As discussed earlier, the abnormal measurements varied with the subject. In this section some proposals are put forward to avoid these unwanted conditions.

Software Controlled Program to Detect Sensor Blockage (Fast Sweep Mode)

A software controlled program based on different acquisition patterns has been used to scan the planar array and indicate the pin disrupted due to the bubble or subject's skin. Resolution of the scan can be improved by scanning at +/- 120 degree angles (orange lines) and then the acquired signals can be merged as shown in figure 11 (Beqo N *et al* 2011).

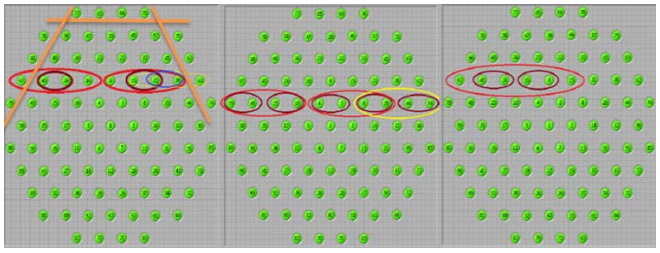

(a) (b) (c)

FIGURE 11. ELECTRODE PLATE AND COMBINATION PATTERNS (BEQO N *ET AL* 2011)

This program was tested by artificially introducing an air bubble on electrode 1 as indicated in figure 12. A flat response is expected if only saline is present in the system which has been experimentally verified as shown in figure 13. With the bubble injected onto electrode 1, the acquisition was made at low frequencies. This resulted in the distortion that can be seen on combination 25 (positive) and 26 (negative), as shown in figure 14.

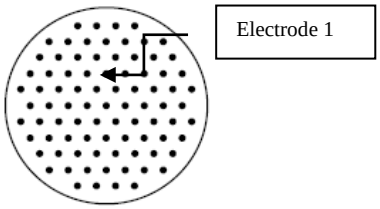

FIGURE 12. ELECTRODE 1 INDICATED

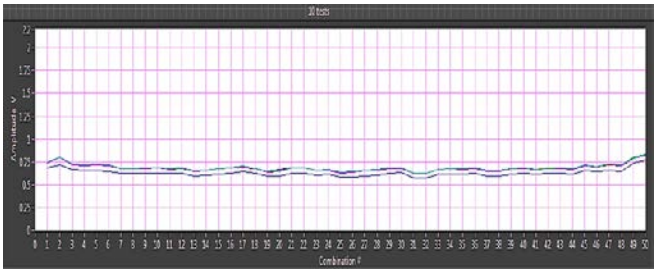

FIGURE 13. FLAT RESPONSE IN SALINE (BEQO N *ET AL* 2011)

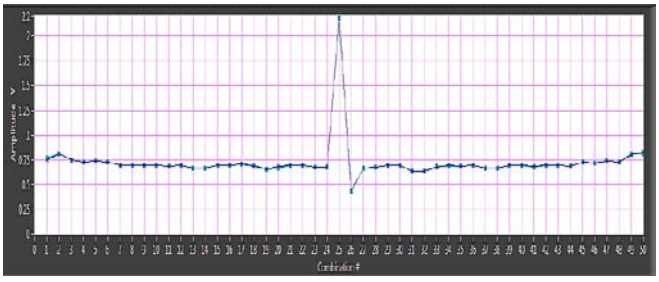

FIGURE 14. OBJECT IDENTIFIED ON ELECTRODE 1 (BEQO N *ET AL* 2011)

The magnitude of the signal can be used to identify to what degree the electrode is covered and/or map

where the breast is touching the electrodes. The 1416 combinations have been reduced to 50, where all the pins alternate into drive and receive using the same distance in every combination. As mentioned above, the scan is done at low frequencies.

By using this dedicated program, the technician managing the patient and system can be notified that the breast needs to be repositioned before scanning, in contrast to a standard acquisition followed by image reconstruction which can take several minutes and so in which there is no quick indicative method to alert the operator. Thus there is no reconstruction involved and the mapping is more or less instant. A mapping example is illustrated below. A party balloon was filled with water and was placed inside the scanner full of saline, as shown in figure 15. The software acquire-map was in continuous mode, at a mapping speed of 4 seconds per scan. The balloon was moved around the scanner to determine that the map signature corresponding to the new position, as shown in figure 16.

The scan takes only a few seconds and provides almost real-time feedback on the electrode functionality. Taking into consideration the amount of time it takes for a full acquisition and reconstruction, this dynamic scan method can help considerably in patient positioning (Beqo N *et al* 2011).

FIGURE 15. WATER FILLED BALLOON IN THE SCANNER

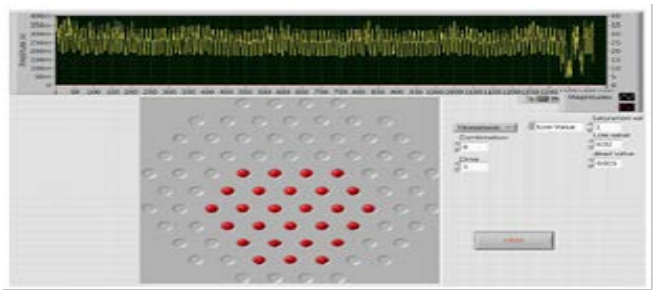

FIGURE 16. BALLOON MAP WITH FAST ACQUISITION (BEQO N *ET AL* 2011)

Dry Skin Minimisation

The subject is properly moistened before scanning in order to avoid bubbles being generated through air trapped in the fine hair of the skin. Baby wipes can be used to moisten the skin before scanning. The non-conductive and non-adhesive nature of the wipes will not contribute any disruption to the acquired signal(Grimnes and Martinsen 2008).

Reducing Saline Displacement Due to Skin and Weight

The hypothesis of disruption due to saline displacement by the breast was verified by an experiment performed with the transparent water filled balloon shown in figure 15. Though non-conductive in nature, the transparent balloon is only used to study the effect of displacement caused by the subject skin and weight. It is observed that the surface contact and weight of the balloon removes the contact medium by displacing the saline from the electrodes.

Systematic Error Mitigation

Systematic errors such as electrolysis and sensor configuration can be minimised by using degassed water saline solution along with rinsing of the electrodes with a non-conductive, high surface tension liquid. This prevents bubbles forming or staying on the electrodes due to micro gaps between the plate and the electrodes. For the Sussex Mk 4 EIM system, cholorohexidine with 155μS of conductivity is used for this purpose,that is to avoid bubble formation and growth.

Sensor configuration errors can arise if there are air pockets between the sensors and the acrylic plate. These air pockets will cause bubbles to accumulate on the sensors and so introduce artefacts during the acquisition. The best possible way of avoiding the artefacts caused by the gaps is to fill in the dry scanner head with saline solution before starting the scanning. Bubbles due to the air pockets between the sensors and the acrylic plate will keep on growing until all of the air pockets are filled. This will minimise the bubble growth and generation due to sensor configuration error.

Reducing Acquisition Scan Time

In order to avoid bubble formation due to DC offset, scanning time per breast should be reduced to deal with the bubble generation problem, so improving overall system performance. Scanning time depends on several factors including: (i) acquiring format used by the controlling (or acquiring) software should be the same as that of the analogue to digital converter (digitiser); (ii) analogue multiplexers with minimum ON and OFF switching time should be employed.

Lateral Scanning Position

In the Sussex Mk 4 System, the scanner head plate moves up and down to accommodate different breast sizes by slightly compressing the breast and holding it steady while the patient lies on her front. The possibility of electrode blockage due to the patient's skin is greater when the breast is pressed against the electrode plate while scanning the volunteer lying on her front, as shown in figure 17. Thus a proposed change of the scanning position is to have the volunteer lie sideways as this will minimise the breast and electrode plate contact. However, lateral scanning will require further investigation (Bilal R *et al* 2011).

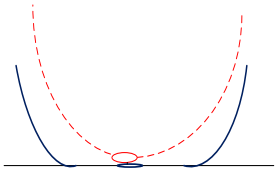

FIGURE 17. COMPARISON OF BREAST MODELS WITH PATIENT LYING ON FRONT (BLUE) AND SIDEWAYS (RED)

Conclusion

From the descriptions presented, it is clear that electrode blockage due to a number of causes such as micro gaps, systematic errors due to bubbles, or the patient's skin covering half or moreof the electrode width will result in unwanted threshold voltage levels. These unwanted levels can be identified by using the electrode combination patterns and a fast sweep method of acquisition. The fast sweep method can thus be a solution to quickly identify any artefact or foreign objects on the electrode pins.

The proposed methodologies presented in this paper will not only prevent the possibility of bubble generation but also electrode blockage due to the patient's skin and so allow a significant improvement of EIM imaging for cancer detection. Future work will optimise the methodologies described for application to a wider range of female populations under different conditions so they may be implemented in the EIM data quality control software routines.

REFERENCES

American Cancer Society 2009, Breast cancer facts & figures 2009-2010.

Barber D C and Brown B H, 1984, Applied Potential Tomography (Review Article), J. Phys.E.: Sci. Instrum. 17 723-733.

Béqo N, Huber N, Bilal R, Zhang W,Qiao G, and Wang W, 2011, Fast method for artefact detectionand breast boundary definition, Journal of Physics: Conference Series 224 012167.

Bilal R, Wang W, Young R, 2011, Analysis and approach to reduce electrode contact artefacts, EIM IEEE EMS 2011, Madrid-Spain, 16-18.

Bilal R, Beqo N, Khan B, Young R, Wang W, 2011, Analysis, Fast method of detection and approach to reduce electrode contact artefacts, EIM IEEE SCOReD 2011, Putrajay-Malaysia.

Boone K G and Holder D S, 1996, Effect of skin impedance on image quality and variability in electrical impedance tomography: a model study, Med. and Biol. Eng. and Comput. 34 (5) 351- 354.

Cheng KS, Isaacson D, Newell J C and Gisser DG,1989, Electrode Models for Electric- Current Computed-Tomography. Ieee Transactions on Biomedical Engineering, 36 (9), 918-924.

Grimnes S and Martinsen Ø G,2008 , Bioimpedance and bioelectricity basics. 2nd ed. ed. London: Academic.

Holder D S, 2005, Electrical Impedance Tomography: methods, history and applications (London:Institute of Physics Publishing).

Hua P, Woo E J, Webster J G, Tompkins W J, 1993, Finite element modeling of electrode-skin contact impedance in electrical impedance tomography, IEEE Trans. Biomedical Engineering 40 (4) 335-343.

Huber N, Béqo N, Adams C, Sze G, Tunstall B, Qiao G, Wang W, 2010, Further investigation of a contactless patient-electrode interface of an Electrical Impedance Mammography system, Journal of Physics: Conference Series 224 012166

Kolehmainen V, Vaukhonen M, Karjalainen P A and Kaipio J P, 1997, Assessment of errors in static electrical impedance tomography with adjacent and trigonometric current patterns, Physiol. Meas. 18 289-303.

McAdams ET, Jossinet J, Lackermeier A and Risacher F ,1996, Factors affecting electrode-gel-skin interface impedance in electrical impedance tomography. Medical & Biological Engineering & Computing, 34 (6), 397-408.

McEwan A,Cusick G, Holder D S, 2007, A review of errors in multifrequency EIT instrumentatio Physiol. Meas., 28

197-215.

Nissinen A, Heikkinen L M, Kolehmainen V and Kaipio J P, 2009, Compensation of errors due to discretization, domain truncation and unknown contact impedances in electrical impedance tomography, Meas. Sci. Technol. 20 (10) 13 pages.

Paulson K, Breckon W and Pidcock M ,1992, Electrode Modeling in Electrical-Impedance Tomography. Siam Journal on Applied Mathematics, 52 (4), 1012-1022.

Rahal M, Khor J M, Demosthenous A, Tizzard A and Bayford R,2009, A comparison study of electrodes for neonate electrical impedance tomography. Physiological Measurement, 30 (6), S73-S84.

Sze G, Wang W, Barber D C , Huber N ,2011, Preliminary study of the sensitivity of the Sussex Mk4 Electrical Impedance Mammography planar electrode system, Journal of Physics: Conference Series 224 012167.

Tunstall B, Wang W, McCormick M, Walker R and Rew D A, 1997, Preliminary in vitro studies of electrical impedance mammography (EIM): a future technique for non-invasive breast tissue imaging?, The Breast 6 (4) 253.

Wang W, Wang L, Qiao G, Prickett P, Bramer B, unstall B and Al-Akaidi M ,2007 ,Study into the repeatability of the electrode-skin interface utilizing electrodes commonly used in Electrical Impedance Tomography. In H. Scharfetter & R. Merwa eds.: Springer Berlin Heidelberg, 336- 339.